Biomedicine & Pharmacotherapy 195 (2026) 119057

Contents lists available at ScienceDirect

Biomedicine & Pharmacotherapy

journal homepage: www.elsevier.com/locate/biopha

Differential effects of the anti-obesity drug tirzepatide on adipose tissues: Brown fat as a key target

Alberto Mestres-Arenas [a,b,c], Tania Quesada-López [a,b,c], Albert Blasco-Roset [a,b,c], Marta Giralt [a,b,c], Francesc Villarroya [a,b,c], Anna Planavila [a,b,c,*], Marion Peyrou [a,b,c,*]

[a] Departament de Bioquímica i Biomedicina Molecular, Facultat de Biologia, Universitat de Barcelona, Institut de Biomedicina de la Universitat de Barcelona (IBUB), Barcelona, Spain
[b] Institut de Recerca de Sant Joan de Déu, Barcelona 08028, Spain
[c] CIBER Fisiopatología de la Obesidad y Nutrición (CIBERobn), Madrid 28029, Spain

ARTICLE INFO

Keywords:
Tirzepatide
brown adipose tissue
mitochondria
adipose tissue
Thermogenesis
Obesity

ABSTRACT

Tirzepatide is an anti-obesity drug based on dual agonism of the incretin receptors GLP-1R and GIPR. Its anti-obesity effect is largely based on its action of reducing food intake. However, there are indications that tirzepatide exerts effects on adipose tissues beyond those resulting from fat loss due to reduced food intake. To investigate this, we treated mice, previously been made obese through high-fat diet, with tirzepatide. We also established an experimental group of mice pair-fed with those treated with tirzepatide, key to distinguish the specific effect of tirzepatide from food intake reduction-mediated effects. Both groups experienced similar reduction in body weight, with a trend toward greater loss in visceral and subcutaneous white fat in mice under tirzepatide treatment. Glucose tolerance improved in tirzepatide-treated obese mice, independently of reduced food intake. Tirzepatide treatment also lowered the inflammatory status of obese mice, which in this case, was attributable to decreased food consumption. Tirzepatide exerted distinct effects on brown adipose tissue relative to white adipose tissues, significantly boosting thermogenic activity and modifying its gene expression pattern, including the upregulation of genes linked to thermogenesis and substrate oxidation. White adipose tissues responded differently, being primarily affected in their lipid metabolism. These effects were specific to tirzepatide treatment and not attributable to reduced food intake. Our results indicate that tirzepatide affects the function and metabolism of adipose tissues and especially induces activation of brown adipose tissue in mice, which may be relevant for future human studies to ascertain the mechanisms of tirzepatide metabolic benefits.

1. Introduction

In recent years, the obesity treatment landscape has advanced significantly with the development of novel drugs targeting incretin receptor pathways. Notably, major progress has been made through the creation of compounds that combine co-agonism of the glucagon-like peptide-1 (GLP-1) and glucose-dependent insulinotropic polypeptide (GIP) receptors within a single molecule [1]. These dual agonists were originally designed to enhance glucose regulation in type 2 diabetes (T2D) by leveraging the additive insulinotropic effects of both pathways, while also amplifying weight loss [1,2]. Currently, tirzepatide (TZP) is the only FDA-approved medication that includes GIP receptor activation, functioning as a dual GLP-1R/GIPR agonist.

Clinical and preclinical studies show that TZP induces greater weight loss than GLP-1R agonists alone, likely due to its combined GLP-1R/GIPR activity [3]. GIPR is more widely expressed than GLP-1R in distinct cells and tissues, including in adipocytes within adipose tissues, which suggests multi-organ sites of action of TZP contributing to its systemic effects on body weight [4,5]. Thus, in animal models, blocking central GIPR abolished appetite suppression but only partly reduced weight loss, implying GIPR acts through both central and peripheral pathways [6]. Only 20 % of TZP's insulin sensitivity benefit is linked to weight loss, unlike GLP-1R agonists, where it's nearly all weight-related [7,8]. Moreover, experimental treatment with TZP reduces

* Corresponding authors at: Departament de Bioquímica i Biomedicina Molecular, Facultat de Biologia, Universitat de Barcelona, Institut de Biomedicina de la Universitat de Barcelona (IBUB), Barcelona, Spain.
E-mail addresses: aplanavila@ub.edu (A. Planavila), marion.peyrou@ub.edu (M. Peyrou).

https://doi.org/10.1016/j.biopha.2026.119057
Received 6 November 2025; Received in revised form 16 January 2026; Accepted 21 January 2026
Available online 26 January 2026

inflammation independently of brain GLP-1R [9]. These findings highlight the need to better understand the mechanisms and sites of action of TZP, beyond its effects reducing food intake.

A particularly important aspect in this context is the potential of TZP to affect adipose tissues. White adipose tissue (WAT) stores excess energy and contributes to fat accumulation under conditions of positive energy balance, leading to obesity. In contrast, the body also contains brown adipose tissue (BAT), which is specialized in adaptive thermogenesis and plays a protective role against obesity [10,11]. Adipose tissue is highly plastic, and the so-called beige adipocytes, i.e. thermogenic adipocytes resembling brown adipocytes, can emerge within WAT in conditions of thermogenic stimulus [12].

The direct and indirect actions of incretin-based anti-obesity drugs, which modify the properties of adipose tissue, are emerging as key contributors to the systemic health benefits of these treatments. Multiple studies have reported that GLP-1 receptor agonism may affect WAT metabolism and it has been proposed to enhance brown and beige fat activity indirectly, primarily through central nervous system mechanisms that activate the sympathetic nervous system, as well as through effects on immune cells within adipose depots [13]. GIP receptor agonism, in turn, appears to have a more direct capacity to affect WAT lipid and glucose metabolism and to promote its thermogenic remodeling by acting on adipocytes and other cell types within adipose tissue [13]. Given the dual GLP-1R and GIPR agonism present in TZP, its effects on adipose tissues could help explain the superior weight loss effects of TZP compared to single GLP-1 receptor agonists. A few experimental studies have addressed directly the effects of TZP on adipose tissues and found that TZP increases glucose disposal in WAT, enhances catabolism in BAT and modulates the regulation of nutrient metabolism of white adipocytes [4,14]. In the current study, we conducted a comprehensive analysis of the effects of TZP on distinct adipose depots using an experimental mouse model. While this experimental model has inherent limitations in relation to human health, it allowed us to use invasive tissue analysis that helped us elucidate the specific effects of TZP on different adipose tissue depots and identify BAT as a key target of TZP action.

2. Materials and methods

2.1. Mouse experimentation

C57BL/6 J male mice were obtained from Harlan Laboratories (Indianapolis, IN, USA). At 5 weeks of age, the mice were placed on a high-fat diet (HFD; #D12451, 45 % kcal from fat, Envigo, VA, USA) for 15 weeks, by which time they had developed obesity, defined as a 150 % increase in body weight compared to standard diet-fed controls. Following the 15-weeks HFD period, obese mice received treatment with a hydrosoluble TZP (AdipoGen life sciences, Fuellinsdorf, Switzerland). TZP was administered daily during 12 days via intraperitoneal (i.p.) injections at a dose of 10 nmol/kg for 5 days (corresponding to 48 μg/kg), followed by 20 nmol/kg (corresponding to 96 μg/kg) for an additional 7 days. TZP powder was diluted in saline to a concentration of 17 μg/ml. Volume of injection was in a range between 80 μl to 130 μl adapting to every mice weight prior to treatment. Control mice received saline injections with a volume in a range between 80 μl to 130 μl, adapting to every mice weight prior to treatment. A pair-fed (PF) control group, receiving the same amount of HFD consumed daily by the TZP-treated group and saline injections, was also included. To that end, each mouse of the TZP group was paired with a mouse displaying similar body weight prior to treatment. Food consumption was monitored individually for each animals of the TZP group and supplied for PF group once a day in the morning. For glucose tolerance tests, mice were fasted for 6 h and injected by i.p. with glucose (2.5 g/kg in aqueous solution). Surface temperature at the interscapular BAT site was assessed by infrared thermography, in the morning, at an ambient temperature of 22ºC, 24 h after manual shaving of approximately 6 cm^2 of the dorsal area in mice under light anesthesia with isoflurane. The region of interest (ROI) was defined as a circular area of approximately 1 cm in diameter, centered on the interscapular depression. The maximum temperature within this area was measured using a T335 digital infrared camera (FLIR Systems, Wilsonville, OR, USA) positioned 30 cm away at an angle of less than 10° from the perpendicular as described before [15]. 1 picture per animal (7 animals per group) were analyzed with FLIR Quick Report 1.2 software.

At the end of the experiment, mice were anesthetized and sacrificed by decapitation. Tissues were rapidly dissected and snap-frozen in liquid nitrogen for further analysis. Blood was collected for plasma separation and subsequent analyses. All experiments were performed in accordance with European Community Council directive 86/609/EEC, and experimental protocols as well as the number of animals, determined based on the expected effects size, were approved by the Institutional Animal Care and Use Committee at the University of Barcelona.

2.2. Analysis of circulating parameters

Blood glucose and triglyceride levels were measured using an Accutrend System (Roche Diagnostics GmbH, Mannheim, Germany). Non-esterified fatty acid (NEFA) levels were quantified using NEFA-HR kit (Fujifilm, Barcelona, Spain) and glycerol levels were determined using free glycerol reagent kit (Sigma-Aldrich, Madrid, Spain). Affinity-based proteomics analysis of plasma was performed using the Olink Mouse Exploratory Target 96 panel (Thermo Fisher Scientific) and employing the COBIOMIC Biosciences laboratory (COBIOMIC, Córdoba, Spain). Quantified proteins were selected for extracellular annotation according to The Human Protein Atlas (https://www.proteinatlas.org), and the Olink functional categorization of proteins based on UniProt, KEGG, Gene Ontology, and STRING databases was used, with minor modifications. Mouse adipokine-endocrine "Multiplex Assay" (Merck Millipore, MADKMAG-71K-05) was performed using a Luminex 100 IS version 2 equipment (Luminex, Austin, TX, USA). Mouse adiponectin ELISA kit (Invitrogen, Madrid, Spain) was used to determine adiponectin levels in blood.

2.3. Histology

Tissues were fixed overnight in 4 % paraformaldehyde, sectioned at 5 μm thickness, and stained with hematoxylin and eosin (H&E) for morphological examination. Tissue processing was carried out by the HCB-IDIBAPS Biobank (B.0000575), part of the ISCIII Biobanks platform, in collaboration with Biomodels. The lipid surface area was quantified with Image J 2.0 (NIH) using the panel Image > Adjust > Threshold, as described in [16].

2.4. RNA analyses

RNA was extracted from adipose tissues using a NucleoSpin RNA column kit (Macherey-Nagel). Reverse transcription of 0.5 μg of total RNA in a total reaction volume of 20 μL was performed using a high-capacity complementary DNA (cDNA) kit. Samples were systematically checked for null amplification in the absence of reverse transcriptase. qRT-PCR was performed using TaqMan probes (Supplementary material); each 20 μL reaction mixture contained 1 μL cDNA, 10 μL TaqMan Universal PCR Master Mix (Thermo Fisher Scientific) and 250 nM probes. The cDNA level of each gene of interest was normalized to that of a housekeeping reference gene (*Ppia* mRNA). The comparative CT ($2^{-\Delta Ct}$) method was applied for normalization. RNAseq data was obtained with the support of Novogene (Cambridge, United Kingdom). Sample RNA concentration, purity, and integrity (RIN) were assessed and mRNA was purified from 400 ng total RNA input material using poly-T oligo-attached magnetic beads. After fragmentation, the first strand cDNA was synthesized using random hexamer primers, followed by the second strand cDNA synthesis. The library was

ready after end repair, A-tailing, adapter ligation, size selection, amplification, and purification. The library was checked with Qubit (Thermo Fisher Scientific), quantified by RT-PCR, and bioanalyzed for size distribution detection. Quantified libraries were pooled and sequenced on Illumina platforms (Illumina, Foster City, CA, USA) according to effective library concentration and data amount. Bulk data were retrieved, and clean reads were mapped to the *Mus musculus* reference genome GRCm39/mm39 using HISAT2 software version 2.2.1 [17]. Then, gene expression was quantified and normalized using the R package DESeq2 version 1.24.0, considering library size and composition. DESeq2 normalized data were used to calculate principal components affecting sample distribution. The visualization of the two main principal components was performed using the R package BiocGenerics version 0.54.0. Likewise, pairwise correlation values for each sample were computed taking the log-transformed numerical matrix and correlated with the R package stats:cor version 3.6.2. Differential expression analyses between experimental conditions were conducted with DESeq2. For each gene, the log2 fold change and a Fisher's exact test *P* -value corrected by a 5 % false discovery rate were calculated. Differential expression was estimated upon an adjusted *P* -value cutoff of $P < 0.05$. Next, differentially expressed genes were employed to perform functional enrichment annotation analyses and assess pathways affected between experimental conditions. The R package enrich R version 3.4.0 with annotated Gene Ontology terms for *Mus musculus* was applied to the list of differentially expressed genes and biological pathways enrichment analysis performed using Kyoto Encyclopedia of Genes Genomes (KEGG), Gene Ontology (GO) and Reactome database tools. Raw-count datasets for the expression of each gene and individual transcript are available at the EMBL's European Bioinformatics Institute EMBL-EBI ArrayExpress (EMBL-EBI accession: E-MTAB-15994). RIN, mapping rates, read counts, list of top up-regulated BAT genes, gene sets and principal component analysis are available in Supplementary Fig. 4. For comparison of the transcriptome changes elicited by TZP treatment in BAT and those caused by cold-induced thermogenic activation of BAT, the publicly available dataset GSE198046 was used [18].

2.5. Protein analyses

Homogenized tissues were lysed in ice-cold RIPA buffer. Equal amounts of protein were separated by sodium dodecyl sulfate-polyacrylamide gel electrophoresis (SDS-PAGE) on 12 % or 15 % gradient gels and blotted onto PVDF (polyvinylidenedifluoride) membranes. Proteins were probed with specific primary antibodies (dilution 1/1000 for UCP1 and TOM20 antibodies and 1/5000 for OXPHOS antibodies) and HRP-conjugated secondary antibodies (dilution 1/3000 for UCP1 and TOM20 antibodies and 1/20000 for OXPHOS antibodies) in combination with chemiluminescence detection. Loading controls were established using Ponceau staining for each membrane. Each protein was normalized with its correspondent Ponceau staining. Quantification was performed using Multi Gauge V3.0 Software (Fujifilm, Tokyo, Japan).

2.6. Statistical analysis

Data are presented as mean ± SEM from a minimum of four animals per group. Statistical significance was assessed using two-way analysis of variance (ANOVA), followed by Tukey's multiple comparisons test when more than two groups or multiple time points were involved. Analyses were performed using GraphPad software (GraphPad v9.0 Software Inc., San Diego, CA, USA). Differences were considered statistically significant at $P < 0.05$, with individual *P*-values indicated in the figure legends.

3. Results

3.1. Effects of TZP treatment on body weight, food intake and glucose homeostasis in obese mice

Daily treatment of HFD-induced obese mice with 10 nmol/kg/day of TZP (Fig. 1A) resulted in a progressive reduction in body weight, which plateaued at approximately 90 % of the initial weight by day 5 following treatment initiation (Fig. 1B). This weight loss was accompanied by a marked reduction in food intake, which dropped to about one-third of that observed in untreated mice shortly after treatment began (Fig. 1C). After five days, food intake began to recover, coinciding with the stabilization of body weight. To mimic the therapeutic dosing escalation commonly used in clinical settings, the TZP dose was increased to 20 nmol/kg/day after day 5. This led to a further reduction in body weight, reaching approximately 80 % of the initial weight one week after treatment began. A renewed decrease in food intake was observed following the second dose escalation (Fig. 1B and C). In parallel, a third group of pair-fed, non-treated mice was included. Their food intake was matched daily to that of the TZP-treated group throughout the treatment period. These pair-fed mice exhibited a nearly identical body weight loss profile to that of the TZP-treated mice, indicating that most of the weight loss induced by TZP is attributable to reduced food intake (Fig. 1B and C).

At the end of the treatment period, TZP-treated mice showed significantly lower blood glucose levels compared to both untreated HFD-induced obese mice and pair-fed obese controls (Fig. 1E). Additionally, only the TZP-treated group exhibited a significant reduction in triglyceride levels (Fig. 1F). The levels of NEFAs and glycerol were reduced in the plasma of TZP treated mice, confirming reduced adipose tissue lipolysis (Figs. 1G and 1H). Notably, TZP-treated mice showed a marked improvement in glucose tolerance as shown by reduced incremental area under the curve (iAUC) in glucose tolerance tests, whereas only a mild effect was observed in the pair-fed group (Fig. 1D). These findings confirm that TZP exerts specific metabolic benefits in obese mice that go beyond the effects of reduced food intake and weight loss.

3.2. TZP treatment reduces lipid accumulation in white adipocytes and enhances thermogenic activity in BAT

Adipose tissues analysis at the end of the treatment revealed a significant reduction in the size of the inguinal WAT depot (representing subcutaneous WAT), epididymal WAT (representing visceral WAT), and BAT in TZP-treated mice compared to control obese mice. In contrast, the pair-fed group did not show significant reductions in adipose tissue depot sizes; however, their values were intermediate between those of the TZP-treated and ad libitum-fed control mice (Fig. 2A).

Histological analysis revealed a significant reduction in the average adipocyte size in both iWAT and eWAT depots of TZP-treated mice compared to controls (Fig. 2B). Pair-fed mice did not show a significant decrease in adipocyte size. In BAT, TZP treatment led to a marked reduction in the size of lipid droplets (Fig. 2B) within brown adipocytes, relative to untreated, ad libitum-fed obese mice. Pair-fed mice exhibited a modest trend toward decreased lipid droplet content, though the effect was notably less pronounced than in the TZP-treated group. These findings underscore that TZP exerts significant effects on adipose and lipid storage, which cannot be explained solely by reduced food intake.

Infrared-based analysis of skin temperature over the interscapular BAT depot, a surrogate measure of BAT activity, was performed. The data showed that pair-feeding (i.e., food restriction alone) led to a reduction in BAT thermogenesis. In contrast, TZP treatment in the context of the same level of food restriction resulted in a significant increase in BAT thermogenic activity compared to pair-fed mice, reaching levels comparable to those of ad libitum-fed controls. (Fig. 2C). These findings suggest that TZP treatment counteracts the known decline in BAT activity induced by caloric restriction.

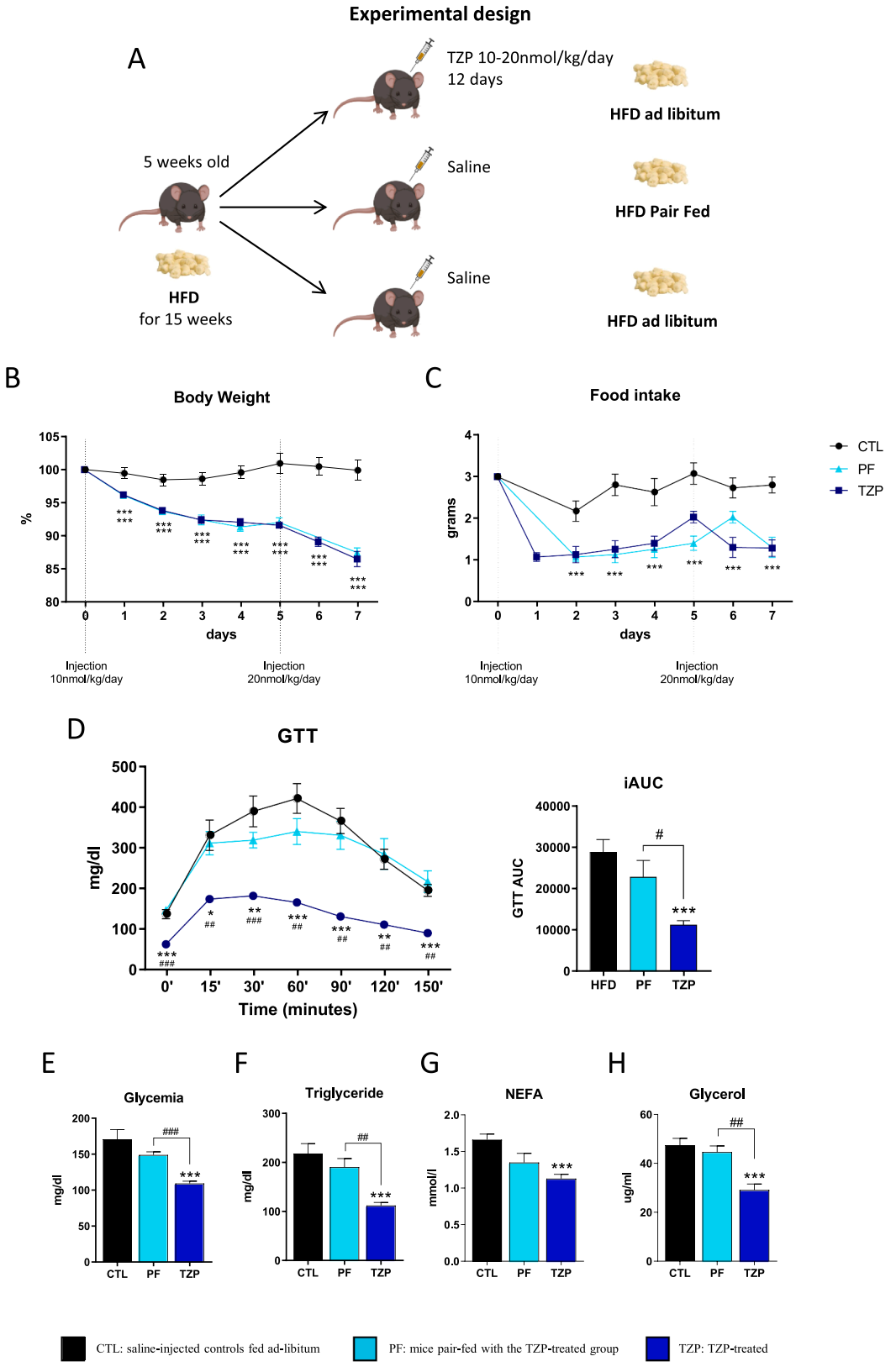

Fig. 1. TZP treatment reduces body weight and improves glucose tolerance in obese mice. A) Schematic representation of experimental design. B) Body weight curve during TZP/saline treatment (day 0–5 10 nmol/kg/day, day 6–12 20 nmol/kg/day). C) Food intake curve during the first week of TZP/saline injection. D) Glucose tolerance test performed at day 8 of TZP/saline treatment and increment area under the curve (iAUC). E) Fasted basal glycemia and triglyceridemia (F). G) Plasmatic levels of non-esterified fatty acids (NEFAs) and glycerol (H). Data are presented as means ± s.e.m. $^{*}P < 0.05$, $^{**}P < 0.01$ and $^{***}P < 0.001$ for TZP vs CTL and PF vs CTL. $^{\#}P < 0.05$, $^{\#\#}P < 0.01$ and $^{\#\#\#}P < 0.001$ for TZP vs PF. (N = 7 animals per group). *P*-values were determined by two ways ANOVA with Tukey's post hoc test for B-C and E- H and repeated measures for D.

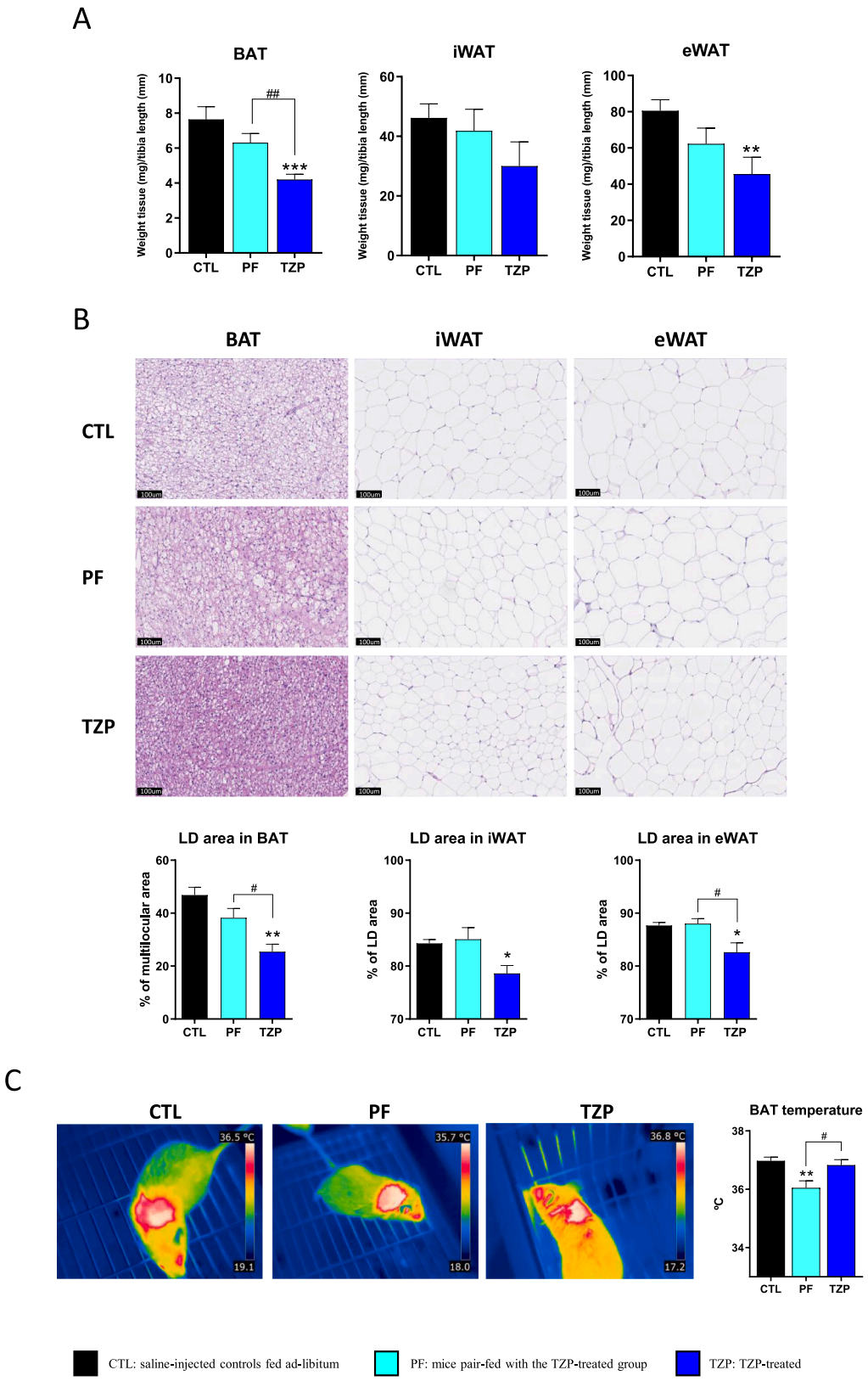

Fig. 2. TZP treatment in obese mice reduces lipid droplets size in fat depots and increases BAT temperature. A) Weight of BAT, iWAT and eWAT tissues normalized with tibia length. B) Representative H&E-stained histological sections of BAT, iWAT and eWAT of mice injected daily with TZP or saline for 12 days, and percentage of lipid droplet area quantification. C) Representative thermography images (left) and quantification of BAT temperature (right). Data are presented as means ± s.e.m. $^{*}P < 0.05$, $^{**}P < 0.01$ and $^{***}P < 0.001$ for TZP vs CTL and PF vs CTL. $^{\#}P < 0.05$ and $^{\#\#}P < 0.01$ for TZP vs PF. (N = 7 animals per group). *P*-values were determined by two ways ANOVA with Tukey's post hoc test.

3.3. TZP treatment reduces systemic inflammation in obese mice

To further investigate the systemic effects of TZP that may contribute to improvements in obesity-related metabolic dysfunction, an unbiased, affinity-based proteomics analysis of plasma was performed. This approach allows for the quantification of low-abundance circulating factors. Of the 58 extracellular proteins quantified, six showed significant changes in TZP-treated mice (see Supplementary Fig 1 and Supplementary table 1). When protein concentration changes were categorized into functional groups using the Olink classification, the "inflammatory/immune" and "enzyme" categories were the most affected by TZP treatment (Fig. 3A, Supplementary Fig 1). The changes observed in the "enzyme" category reflected a trend toward down-regulation of enzymes such as lipoprotein lipase and perilipin-1, which play key roles in lipid metabolism within adipose tissue. The effects on "inflammatory/immune"-related proteins were particularly associated with reduced circulating levels of pro-inflammatory cytokines and chemokines, including interleukin-1α, interleukin-1β, and chemokine (CC motif) ligand 5 (Supplementary Fig 1). Further analysis of plasma using a targeted multiplex cytokine analysis indicated that TZP treatment caused a significant reduction in tumor necrosis factor-α, interleukin-6 and monocyte chemoattracting protein-1 (Ccl2) circulating levels (Fig. 3B). This decrease was similarly found in pair-fed mice. Overall, these results underscore an anti-inflammatory effect of TZP treatment, largely mediated by the reduction in food intake, which may play a role in ameliorating the pro-inflammatory state associated with obesity. Interestingly, leptin levels were down-regulated in the TZP-treated mice but not in pair-fed mice, consistent with the significant reduction in eWAT size and the similar trend observed in iWAT size only in the TZP-treated group. Finally, the levels of adiponectin remained unchanged (Fig. 3B).

3.4. Differential transcriptomic changes in response to TZP treatment in adipose tissues

To gain a comprehensive understanding of the effects of TZP treatment on adipose tissues, whole-transcriptome RNA sequencing was performed. The analysis revealed 1053 differentially expressed genes (DEGs) in BAT (426 upregulated and 627 downregulated), 525 DEGs in eWAT (123 up- and 402 downregulated), and 890 DEGs in iWAT (336

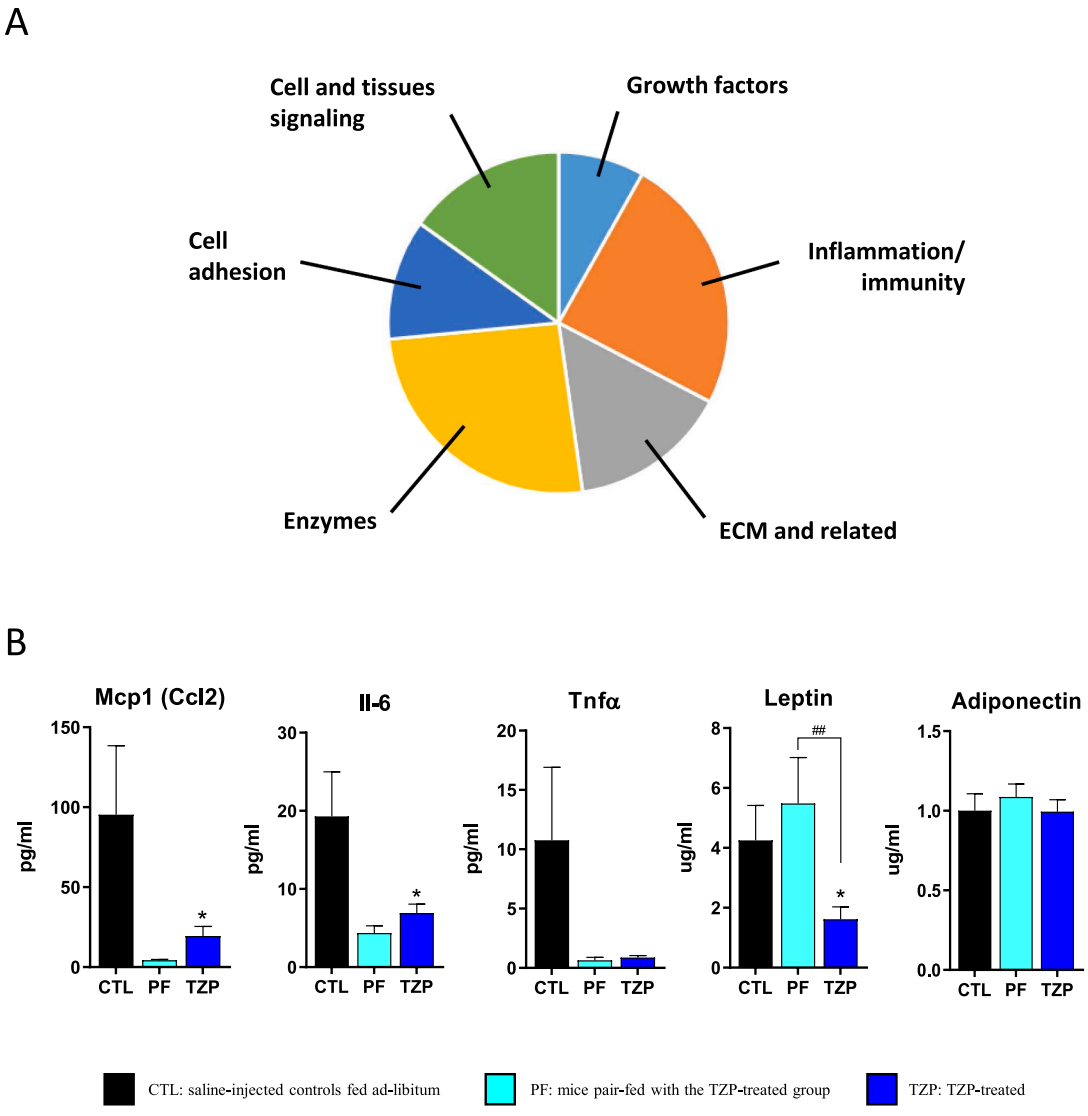

Fig. 3. TZP treatment reduces systemic inflammation in obese mice. A) Representation of the functional categories associated with changes in plasma protein levels of TZP-treated mice compared with saline-injected controls, as determined by affinity-based proteomics (Olink). B) Blood levels of pro-inflammatory cytokines, leptin and adiponectin, as determined by Multiplex and ELISA. Data are presented as means ± s.e.m. $^{*}P < 0.05$ for TZP vs CTL. $^{\#}P < 0.05$ and $^{\#\#}P < 0.01$ for TZP vs PF. (N = 5 animals for A and between 4 and 12 animals per group in B). *P*-values were determined by two ways ANOVA with Tukey's post hoc test.

up- and 554 downregulated) (Supplementary Fig 2, Volcano plots). These DEGs were subjected to KEGG and GO pathway enrichment analysis to identify the biological pathways affected by TZP treatment. In BAT, the top pathway affected by TZP was "thermogenesis", with "oxidative phosphorylation" also ranking among the most significantly enriched in KEGG analysis, and this was confirmed by GO analysis of biological processes and molecular functions which revealed a uniquely distinct profile (Fig. 4A, B). 24 out of the top 30 enriched GO terms were related to mitochondrial respiration and biogenesis (Fig. 4B). To confirm these findings, we compared that profile of changes in the BAT transcriptome caused by TZP treatment with those elicited by activation of BAT through the classical thermogenic stimulus of cold exposure, as previously described [18]. Among the genes induced by TZP close to 20 % overlapped with those induced by the thermogenic stimulus of ten days cold exposure. KEGG analysis revealed that these genes were annotated for "Thermogenesis" and "Oxidative phosphorylation" (the latter corresponding to genes related to mitochondrial function, for which KEGG also generates identification of pathways related to several neurodegenerative diseases) (Fig. 4C). Regarding genes which expression was repressed in BAT by TZP treatment, about 15 % overlapped with those repressed by cold in BAT (Fig. 4D). In this case, the most affected pathway was "Complement and coagulation cascade", a pathway known to be involved in BAT thermogenic regulation according to several previous studies [19]. Overall, these findings support a robust thermogenic activation of BAT in response to TZP.

On the other hand, the results revealed a striking similarity in the pathways altered in the two WAT depots (iWAT and eWAT), while BAT exhibited a distinctly different pattern. Among the top 20 KEGG pathways impacted by TZP in WAT, eight were commonly enriched, including those related to lipid metabolism (e.g., "arachidonic acid metabolism", "linolenic acid metabolism" "PPAR signaling"), "retinoid metabolism", and pathways associated with insulin sensitivity (e.g.,"PI3K-Akt signaling"), as well as those involving the extracellular matrix (Fig. 5A, B). GO analysis confirmed these observations as TZP treatment was shown again to lead to overlapping changes in iWAT and eWAT, particularly in lipid and lipoprotein metabolism and extracellular matrix/collagen homeostasis. A specific enrichment in iWAT (but not eWAT) was noted for terms related to lymphocyte differentiation and epigenetic regulation, indicating depot-specific responses (Fig. 5B). Notably, only two KEGG pathways, "fat digestion and absorption" and "complement and coagulation cascades", were commonly affected across WAT and BAT. Interestingly, thermogenesis did not emerge as an enriched pathway in iWAT, despite its known browning capacity, unlike eWAT. To complement the KEGG and GO findings, an independent Reactome pathway analysis was performed (Supplementary Fig 3). This analysis reinforced the overlap between iWAT and eWAT responses, with 9 out of the top 20 pathways commonly enriched. Many of these involved extracellular matrix regulation, particularly collagen remodeling and matrix degradation. In contrast, BAT again showed a distinct response, with 10 of the top 20 Reactome pathways linked to mitochondrial bioenergetic processes, such as the "electron transport chain", "TCA cycle", and several processes related to mitochondrial DNA function, further supporting enhanced BAT thermogenic activity (Supplementary Fig 3).

3.5. TZP treatment activates thermogenic oxidative pathways in BAT and alters lipid metabolism in WAT depots independently of its food intake-suppressing effects

To validate these findings and determine the extent to which the effects of TZP on adipose tissue gene expression are independent of reduced food intake, we conducted a targeted analysis of transcript levels for key thermogenic marker genes in BAT and WAT depots. This analysis was performed in obese mice treated with TZP, untreated obese control mice, and pair-fed mice.

The results revealed a significant upregulation of *Ucp1*, *Dio2*, and *Ppargc1a*, well-established regulators of thermogenesis [10], as well as *Bmp8b* and *Cxcl14*, two known batokines [20], in BAT from TZP-treated mice (Fig. 6A, left). Interestingly, *AdipoQ* expression gene was increased by TZP even though this was not reflected at systemic level (Fig. 3B). Furthermore, the expression of genes encoding components of the mitochondrial respiratory chain and oxidative phosphorylation pathways, both nuclear- and mitochondrial genome-encoded, was consistently elevated (Fig. 6A, right). These changes were observed exclusively in the BAT of TZP-treated mice and were absent in pair-fed controls. In contrast, no significant alterations in the expression of thermogenic or mitochondrial genes were detected in iWAT or eWAT under either TZP or pair-fed conditions (Fig. 6B, C). These findings confirm that TZP enhances thermogenic activity specifically in BAT through mechanisms independent of its effects on food intake. We also examined gene expression in WAT depots for pathways previously identified by RNAseq to be modulated by TZP treatment. In iWAT, TZP treatment induced upregulation of genes involved in lipid metabolism, including *Scd1*, *Fabp1*, *Acox1*, *Cpt2*, *Lpl*, *Plin1* and *Plin2*, an effect not seen in pair-fed mice (Fig. 6B). No such gene expression changes were observed in eWAT (Fig. 6C). Analysis of transcripts associated with ECM remodeling, including various collagen subtypes and *Tgfb1*, showed no meaningful differences in iWAT (Fig. 6B). Expression of some collagen subtypes was up-regulated (*Col3a1*, *Col1a1*) or down-regulated (*Col12a1*) in eWAT from TZP-treated mice suggesting some affectation of the ECM (Fig. 6C).

3.6. TZP treatment increases UCP1 and mitochondrial respiratory chain/oxidative phosphorylation-related protein levels in BAT

To confirm the key findings related to the pronounced effects of TZP on the thermogenesis-associated transcriptome in BAT, we analyzed protein components involved in the thermogenic and mitochondrial oxidative metabolism in BAT (Fig. 7). Data indicated that TZP treatment increased UCP1 levels as well as respiratory complex subunits SDHB (Complex II) and COXI (Complex IV) protein levels. This effect was observed exclusively in TZP-treated group for UCP1 and SDHB, but also in the pair-fed group for COXI, indicating that reduced food intake partially contributed to the effects observed in the TZP-treated mice. Moreover, TZP treatment increased the TOM20 protein levels, indicating that TZP may enhance mitochondrial mass in BAT.

4. Discussion

TZP treatment is a potent anti-obesity intervention that leads to significant body weight loss, primarily through reduced food intake [2]. However, emerging evidence suggests that TZP may exert specific effects on adipose tissues beyond the weight loss attributable to decreased caloric intake [13]. In the present study, we aimed to investigate the direct effects of TZP on adipose tissues using an experimental rodent model.

TZP treatment significantly reduced food intake and body weight in mice previously made obese by a HFD. In addition, TZP improved glycemia and glucose tolerance independently of food intake reduction, consistent with the incretin effects of GLP-1 and GIP receptor agonism in TZP [1,2]. Moreover, TZP reduced systemic inflammation and, in this case, the reduction in food intake appears to account for most of this effect. However, our results strongly indicate that TZP affects adipose tissues independently of its weight-reducing effects associated with decreased food intake. Specifically, we found that TZP increases BAT activity, as demonstrated by the induction of thermogenic activity, a marked upregulation of thermogenic gene expression, and enhanced mitochondrial oxidation parameters following treatment. Previous studies have suggested that TZP targets BAT; some of the reported effects were mainly related to changes in catabolic pathways and branched-chain amino acid metabolism within BAT [14,21]. Our findings point to a broader and more direct activation of BAT thermogenesis and oxidative activity. Our current findings pointing to BAT activation

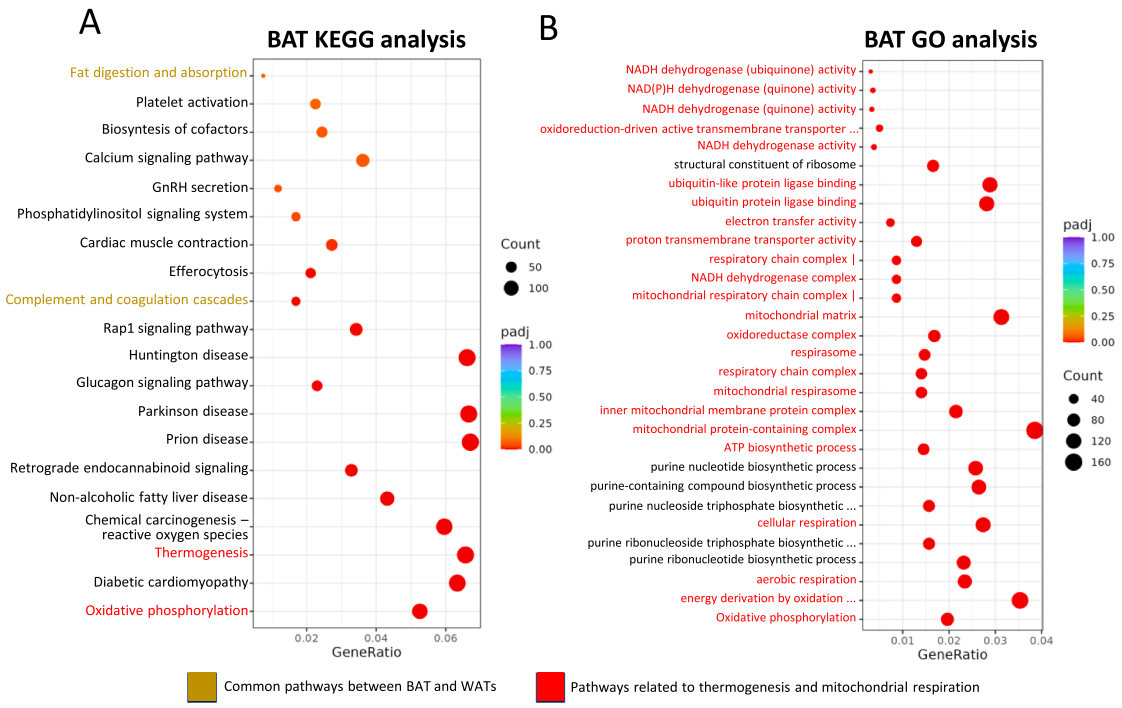

Fig. 4. Thermogenic and mitochondrial oxidation pathways are affected by TZP treatment in BAT. Regulated pathways representation obtained by KEGG (A) and GO (B) analysis of differentially expressed genes according to RNAseq analysis of BAT of obese mice treated with TZP for 12 days relative to saline-injected controls (N = 5 animals per group). Pathways statistical significance was accepted with *P*-values < 0.05. Venn diagrams showing the overlap between genes whose expression is induced (C) or repressed (D) in BAT from TZP-treated mice and those induced (C) or repressed (D) in BAT after 10 days of cold exposure (top), and KEGG analysis of the commonly induced (C) or repressed (D) pathways (bottom). Pathways statistical significance was accepted with adjusted *P*-values < 0.05.

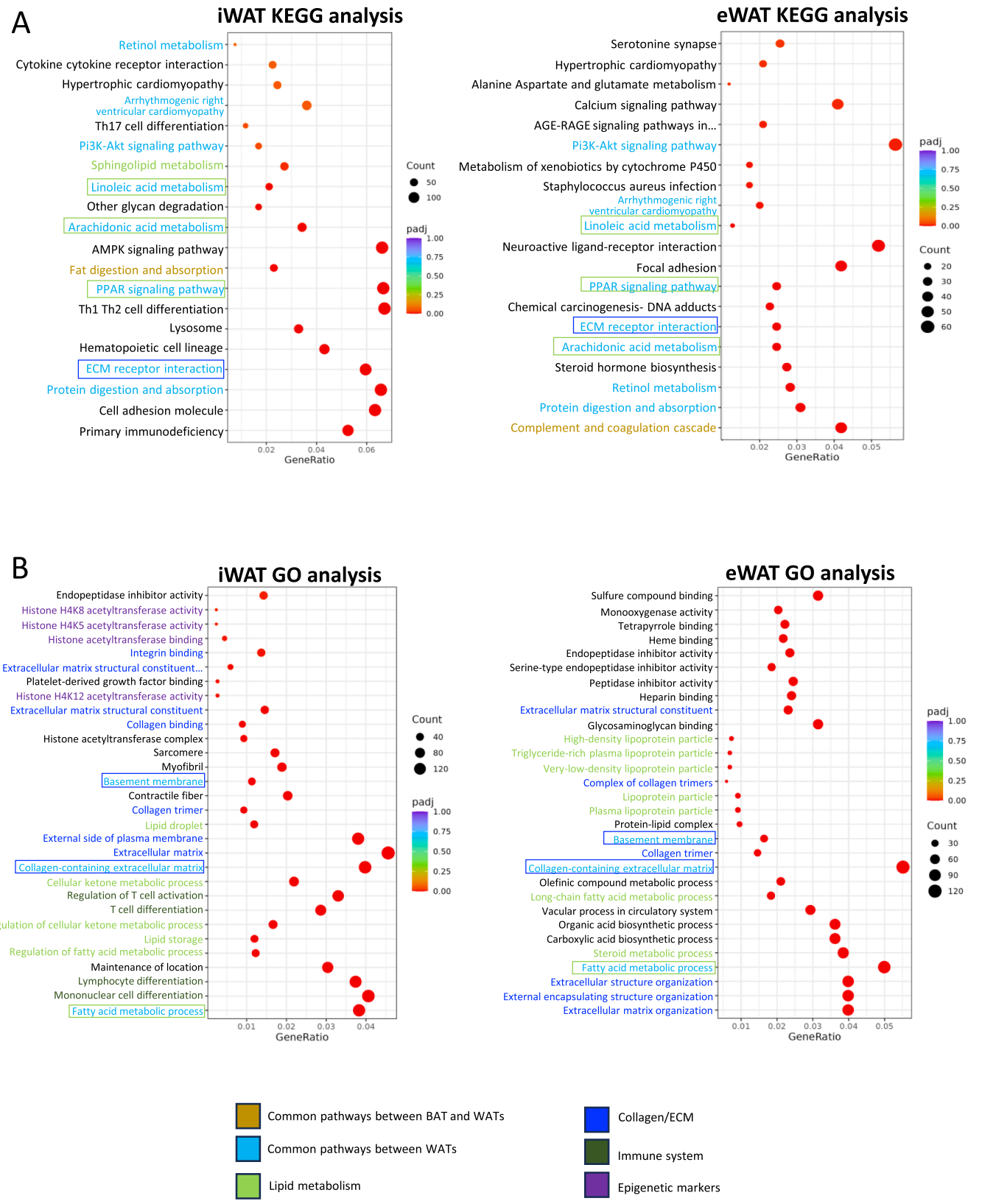

Fig. 5. Lipid metabolism and extracellular matrix pathways are affected by TZP treatment in white adipose tissue depots. Regulated pathways representation obtained by KEGG (A) and GO (B) analysis of RNAseq in iWAT and eWAT of obese mice treated with TZP for 12 days relative to saline-injected controls. (N = 5 animals per group). Pathways statistical significance was accepted with *P*-values < 0.05.

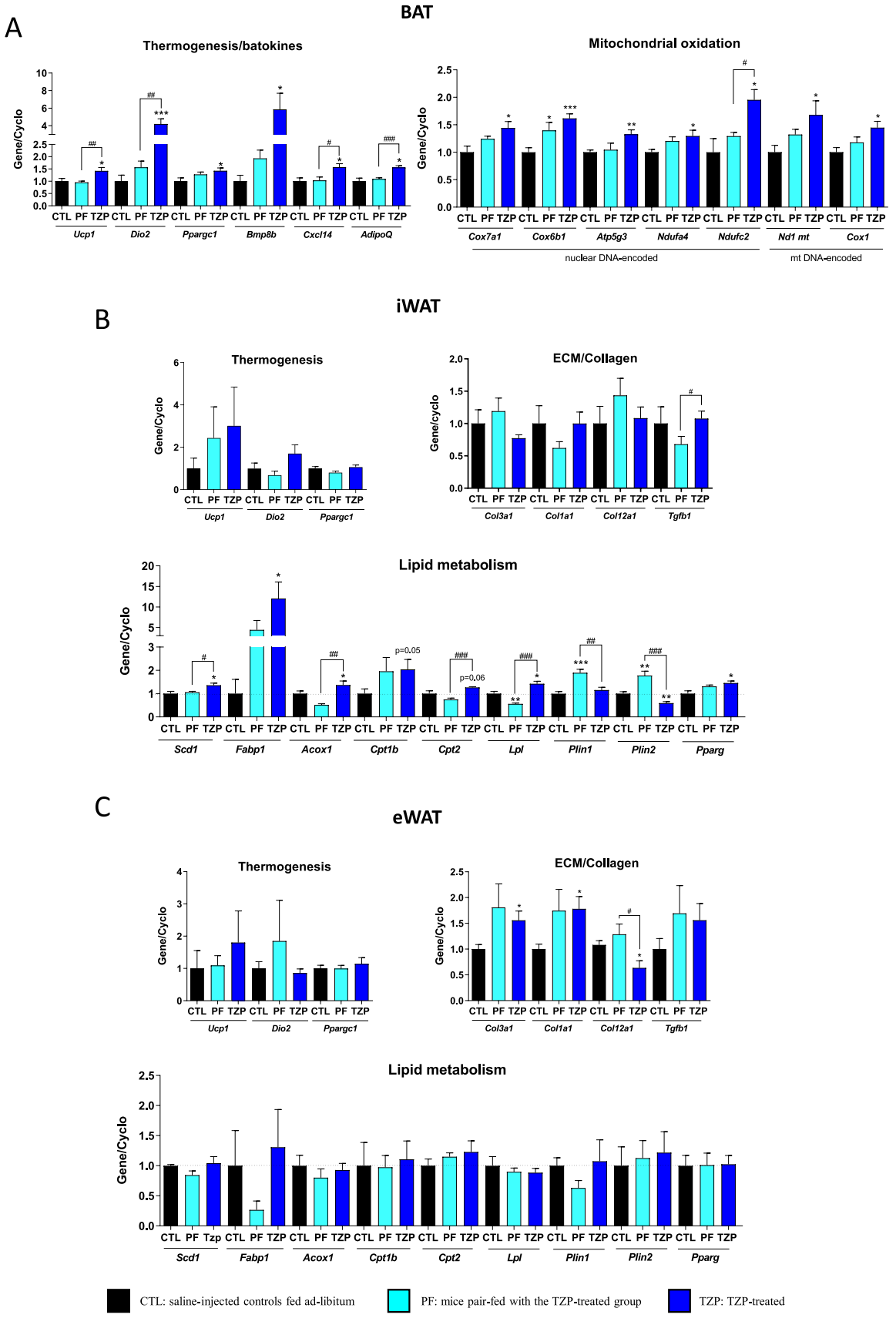

Fig. 6. Gene expression changes in adipose tissues of TZP-treated obese mice in comparison with obese pair-fed mice. mRNA expression of selected genes in BAT (A), iWAT (B) and eWAT (C) of obese mice treated with TZP for 12 days. Data are presented as means ± s.e.m. $^{*}P < 0.05$, $^{**}P < 0.01$ and $^{***}P < 0.001$ for TZP vs CTL and PF vs CTL. $^{\#}P < 0.05$, $^{\#\#}P < 0.01$ and $^{\#\#\#}P < 0.001$ for TZP vs PF. (N = 4–7 animals per group). *P*-values were determined by two ways ANOVA with Tukey's post hoc test.

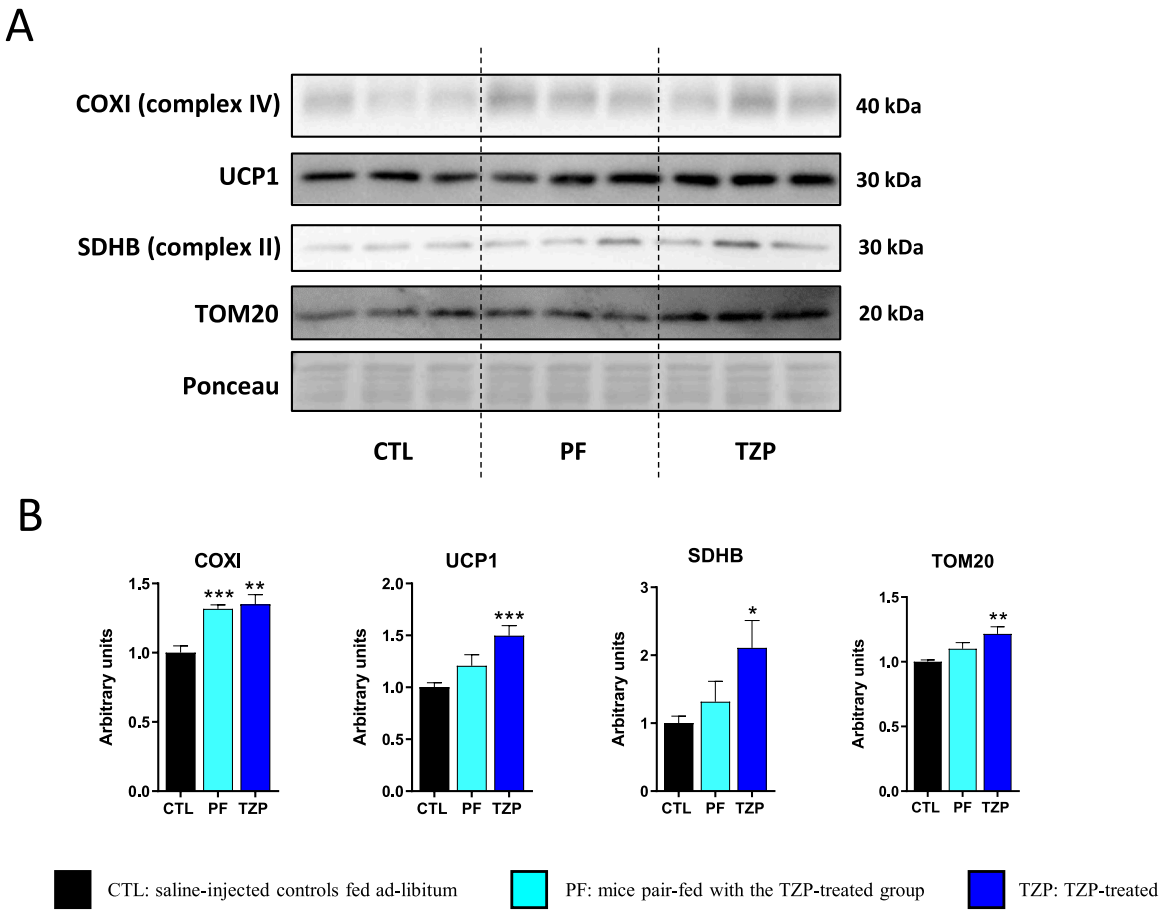

Fig. 7. Mitochondrial proteins are increased by TZP treatment in BAT. A) Representative immunoblots of UCP1, mitochondrial respiratory chain/oxidative phosphorylation-related proteins, and mitochondrial external membrane TOM20 in BAT and quantification (B). Data are presented as means ± s.e.m. $^{*}P < 0.05$ for TZP vs CTL and PF vs CTL. $^{\#}P < 0.05$' for TZP vs PF. (N = 5–6 animals per group). *P*-values were determined by two ways ANOVA with Tukey's post hoc test.

in response to TZP are consistent with previous observations indicating enhanced energy expenditure in mice treated with TZP [22,23], considering the important role of BAT activity in adaptive energy expenditure in rodents. However, we did not find evidence of a massive alteration in energy expenditure in our experimental setting, as TZP-treated mice showed unchanged body weight when food intake was matched. It is possible that TZP-induced BAT activation was not sufficient to influence overall energy balance and is instead more likely involved in regulating specific metabolic processes through substrate utilization, such as glucose, or through the secretory activity of activated BAT and its known systemic metabolic effects [20]. On the other hand, the effects of TZP on BAT may involve both centrally-mediated indirect actions through GLP-1 receptor agonism [24] and more direct effects through GIP receptor agonism, supported by evidence of GIPR expression in distinct brown adipocytes and other cell populations within BAT [25]. Although tirzepatide activates both GIPR and GLP-1R, the adipose tissue-specific nature of the observed molecular changes, together with the known expression of GIPR, but not GLP-1R, in adipocytes [13], suggests a predominant role for GIPR signaling, although indirect GLP-1R-mediated effects cannot be excluded. Recent data point to a key capacity of GIPR activation in BAT to modulate systemic lipid metabolism in mice [26]. Thus, the dual GLP-1R and GIPR agonism characteristic of TZP is likely to underly the observed BAT activation.

In WAT depots, TZP also exerted specific effects that were independent of reduced food intake. These included particularly alterations in lipid metabolism and other metabolic parameters appearing in mice treated with TZP but unrelated to the decrease in food intake. While both eWAT and iWAT depots were affected, the effects were more pronounced in iWAT, suggesting a potentially greater susceptibility of subcutaneous WAT to TZP. The reduction in lipolysis observed in TZP-treated mice, likely reflecting insulin-like actions on adipose tissue, together with the increased expression of fatty-acid oxidation genes (*Acox1, Cpt1, Cpt2*) in iWAT, indicates that TZP promotes fatty-acid oxidation within WAT rather than fatty-acid release, at least in the inguinal depot. In this context, the well-established depot-specific regulation of lipid metabolism between iWAT and eWAT, including the reduced ability of insulin to suppress lipolysis in eWAT compared with iWAT in diet-induced obese mice [27] is consistent with the differential effects of TZP on lipid metabolism in these two adipose depots. However, despite the strong activation of BAT and the known browning potential of iWAT, we did not observe signs of browning in iWAT following TZP treatment. This absence is notable given that iWAT is particularly responsive to browning stimuli. One possible explanation is that the relatively short duration of TZP treatment in our experimental protocol was insufficient to trigger the browning process. Nonetheless, some extent of browning of WAT has been reported to occur within 7–9 days of exposure of diet-induced obese mice to established browning inducers such as cold or β3-adrenergic agonists [28,29]. Therefore, a preferential effect of TZP on activating existing BAT, rather than inducing the browning of WAT cannot be ruled out. Although longer tirzepatide exposure may promote further adipose tissue remodeling, the absence of early browning markers after 12 days, a time frame sufficient for classical pharmacological browning stimuli, such as β3-adrenergic agonist treatment, to induce robust effects, suggests that tirzepatide is not a strong driver of iWAT browning under these conditions. In any case, TZP treatment was able to affect WAT depots

metabolism specifically and independently from reduced food intake given the differences in histological appearance and lipid metabolism gene expression found in TZP-treated mice when compared with pair-fed mice.

Despite the power for invasive analysis of tissue alterations in response to TZP provided by our preclinical model, the current study has the obvious limitation of using a rodent model to advance in a health issue such as how therapy agents act to protect against obesity. Also, the number of mice used in our study was limited in accordance with ethical constraints and animal welfare regulations, although similar group sizes have been previously used in analogous experimental studies [21]. Nonetheless, this should be considered when interpreting the results, particularly for endpoints with smaller effect sizes. Moreover, the important effects of TZP inducing BAT activity reported here should be interpreted within a human context. Some inter-species differences in response to TZP have been reported. First, it appears that the GIPR agonism present in TZP is weaker upon mouse GIPR than human GIPR [30]. Moreover, it has been recently found that, whereas TZP clearly induce energy expenditure in mice (which is markedly consistent with our observation of increased BAT activity), it does not appear to do so in humans despite TZP increase lipid oxidation in patients [13]. However, any potential effects of TZP in human BAT wouldn't necessarily result in increased energy expenditure. BAT activity in humans is not only related to obesity protection but also, independently from body weight changes, in protection against type 2 diabetes and cardiovascular disease [11] likely because of BAT-derived signaling affecting systemic metabolism [20]. In our experimental model, TZP exerted several systemic effects that were distinct from those observed in pair-fed mice, including improved glucose tolerance. It can be hypothesized that, in addition to its incretin effect, TZP-induced BAT activation contributes to these protective outcomes. In any case, the significance in humans of the current observation of a strong BAT activation in mice treated with TZP warrants further research.

There are contradictory data indicating no effect [31] or enhancement [32,33] of BAT activity in response to GLP-1R agonism in humans, and 6 days of subcutaneous GIP infusion can increase the temperature of the supraclavicular area, which is a primary site of BAT depots [34]. However, the effects of TZP as combining GLP-1R and GIPR agonism on BAT have not yet been assessed in humans. The ongoing TABFAT clinical trial focused to ascertain the potential of TZP treatment to enhance BAT activity in women living with obesity using 18F-FDG-PET/CT measurements [35] is expected to provide relevant information in this regard. Thus, assessment of BAT activity in individuals treated with TZP using 18F-FDG–PET/CT, the gold-standard method for quantifying active BAT in humans [36], is warranted to determine the capacity of TZP to activate BAT in humans. In this context, the initiation of the TABFAT clinical trial has reported; although results are not yet available, the study is designed to ascertain the potential of TZP treatment to enhance BAT activity in women living with obesity [35]. Although it remains a very limited practice in human experimental research, the possibility of obtaining BAT biopsies from volunteers could be cautiously considered [37] to further elucidate the effects of TZP on human BAT, where ethically and technically feasible. Given the relative invasiveness of PET/CT scans, complementary approaches may also be employed more extensively in the future, including the less precise but reliable indirect assessments of BAT activity using non-invasive infrared thermography applied to regional BAT depots [38]. These methods may help further expand our understanding of the effects of TZP on human BAT activity.

In conclusion, our pre-clinical study allowed us to identify effects of TZP on adipose tissues distinct from those attributable to its weight reducing impact resulting from reduced food intake. Different adipose depots respond differently to TZP, with BAT activation emerging as a major target of its action. Our study is not without limitations, including the fact that it was conducted only in male mice. Therefore, the need for future studies in females is evident, given the importance of considering potential sex-related differences in the response to TZP and the known sex-dependent variation in BAT activity [39]. Moreover, our findings based on an animal model highlight the need for further research in humans to clarify the potential role of BAT activation in the therapeutic effects of TZP as an anti-obesity drug.

Funding

We thank the State Agency of Research of the Spanish Ministry of Science (MICIN/AEI/10.13039/50110 0011033 and FEDER, EU MCIN (grant PID2023–1467810-I00) for funding. M.P. is a "Ramon y Cajal" researcher (grant RYC2022–037961-I funded by the MCIN/AEI/10.13039/501100011033 and by the European Union Next Generation EU/PRTR).

CRediT authorship contribution statement

Francesc Villarroya: Writing – review & editing, Writing – original draft, Supervision, Funding acquisition, Conceptualization. **Marta Giralt:** Writing – review & editing, Writing – original draft, Supervision, Funding acquisition, Conceptualization. **Marion Peyrou:** Writing – review & editing, Writing – original draft, Visualization, Supervision, Software, Methodology, Investigation, Formal analysis, Data curation, Conceptualization. **Anna Planavila:** Writing – review & editing, Writing – original draft, Visualization, Supervision, Software, Methodology, Investigation, Formal analysis, Data curation, Conceptualization. **Alberto Mestres-Arenas:** Writing – review & editing, Writing – original draft, Visualization, Methodology, Formal analysis, Data curation, Conceptualization. **Albert Blasco-Roset:** Writing – review & editing, Methodology, Investigation. **Tania Quesada-López:** Writing – review & editing, Visualization, Software, Methodology, Investigation, Data curation.

Declaration of Competing Interest

The authors declare that they have no known competing financial interests or personal relationships that could have appeared to influence the work reported in this paper.

Appendix A. Supporting information

Supplementary data associated with this article can be found in the online version at doi:10.1016/j.biopha.2026.119057.

Data availability

Data will be made available on request.

References

[1] C.M. Kusminski, D. Perez-Tilve, T.D. Müller, R.D. DiMarchi, M.H. Tschöp, P. E. Scherer, Transforming obesity: the advancement of multi-receptor drugs, Cell (2024) 3829–3853, https://doi.org/10.1016/j.cell.2024.06.003.

[2] P.J. Rodriguez, B.M. Goodwin Cartwright, S. Gratzl, R. Brar, C. Baker, T. J. Gluckman, et al., Semaglutide vs tirzepatide for weight loss in adults with overweight or obesity, JAMA Intern. Med. 184 (9) (2024) 1056–1064, https://doi.org/10.1001/jamainternmed.2024.2525.

[3] A.Bin Aamir, R. Latif, J.F. Alqoofi, F.A. Almarzoq, J.O. Fallatah, G.A. Hassan, et al., Comparative efficacy of tirzepatide vs. semaglutide in reducing body weight in humans: a systematic review and meta-analysis of clinical trials and real-world data, J. Clin. Med. Res. 17 (5) (2025) 285–296, https://doi.org/10.14740/jocmr6231.

[4] A. Regmi, E. Aihara, M.E. Christe, G. Varga, T.P. Beyer, X. Ruan, et al., Tirzepatide modulates the regulation of adipocyte nutrient metabolism through long-acting activation of the GIP receptor, Cell Metab. 36 (7) (2024) 1534–1549.e7, https://doi.org/10.1016/j.cmet.2024.05.010.

[5] X. Yu, S. Chen, J.-B. Funcke, L.G. Straub, V. Pirro, M.P. Emont, et al., The GIP receptor activates futile calcium cycling in white adipose tissue to increase energy expenditure and drive weight loss in mice, Cell Metab. 7 37 (1) (2024) 187–204.e7, https://doi.org/10.1016/j.cmet.2024.11.003.

[6] Q. Zhang, C.T. Delessa, R. Augustin, M. Bakhti, G. Colldén, D.J. Drucker, et al., The glucose-dependent insulinotropic polypeptide (GIP) regulates body weight and food intake via CNS-GIPR signaling, Cell Metab. 33 (4) (2021) 833–844.e5, https://doi.org/10.1016/j.cmet.2021.01.015.
[7] M.K. Thomas, A. Nikooienejad, R. Bray, X. Cui, J. Wilson, K. Duffin, et al., Dual GIP and GLP-1 Receptor Agonist Tirzepatide Improves beta-cell function and insulin sensitivity in type 2 diabetes, J. Clin. Endocrinol. Metab. 106 (2) (2021) 388–396, https://doi.org/10.1210/clinem/dgaa863.
[8] V.A. Fonseca, M.S. Capehorn, S.K. Garg, E. Jódar Gimeno, O.H. Hansen, A.G. Holst, et al., Reductions in insulin resistance are mediated primarily via weight loss in subjects with type 2 diabetes on semaglutide, J. Clin. Endocrinol. Metab. 104 (9) (2019) 4078–4086, https://doi.org/10.1210/jc.2018-02685.
[9] C.K. Wong, B.A. McLean, L.L. Baggio, J.A. Koehler, R. Hammoud, N. Rittig, et al., Central glucagon-like peptide 1 receptor activation inhibits Toll-like receptor agonist-induced inflammation, Cell Metab. 36 (1) (2024) 130–143.e5, https://doi.org/10.1016/j.cmet.2023.11.009.
[10] B. Cannon, J. Nedergaard, Brown adipose tissue: function and physiological significance, Physiol. Rev. 84 (1) (2004) 277–359, https://doi.org/10.1152/physrev.00015.2003.
[11] T. Becher, S. Palanisamy, D.J. Kramer, M. Eljalby, S.J. Marx, A.G. Wibmer, et al., Brown adipose tissue is associated with cardiometabolic health, Nat. Med. 27 (1) (2021) 58–65, https://doi.org/10.1038/s41591-020-1126-7.
[12] R. Cereijo, M. Giralt, F. Villarroya, Thermogenic brown and beige/brite adipogenesis in humans, Ann. Med. 47 (2) (2015) 169–177, https://doi.org/10.3109/07853890.2014.952328.
[13] F. Villarroya, M. Peyrou, M. Giralt, Adipose tissue, at the core of the action of incretin and glucagon-based anti-obesity drugs, Curr. Obes. Rep. 14 (1) (2025) 67, https://doi.org/10.1007/s13679-025-00660-w.
[14] R.J. Samms, M.E. Christe, K.Al Collins, V. Pirro, B.A. Droz, A.K. Holland, et al., GIPR agonism mediates weight-independent insulin sensitization by tirzepatide in obese mice, J. Clin. Investig. 131 (12) (2021) e146353, https://doi.org/10.1172/JCI146353.
[15] T. Quesada-López, R. Cereijo, J.-V. Turatsinze, A. Planavila, M. Cairó, A. Gavaldà-Navarro, et al., The lipid sensor GPR120 promotes brown fat activation and FGF21 release from adipocytes, Nat. Commun. 7 (2016) 13479, https://doi.org/10.1038/ncomms13479.
[16] P. Domingo, T. Quesada-López, J. Villarroya, M. Cairó, M.D.M. Gutierrez, M. G. Mateo, et al., Differential effects of dolutegravir, bictegravir and raltegravir in adipokines and inflammation markers on human adipocytes, Life Sci. 308 (2022) 120948, https://doi.org/10.1016/j.lfs.2022.120948.
[17] M. Pertea, D. Kim, G.M. Pertea, J.T. Leek, S.L. Salzberg, Transcript-level expression analysis of RNA-seq experiments with HISAT, StringTie and Ballgown, Nat. Protoc. 11 (9) (2016) 1650–1667, https://doi.org/10.1038/nprot.2016.095.
[18] N. Hadadi, M. Spiljar, K. Steinbach, M. Çolakoğlu, C. Chevalier, G. Salinas, et al., Comparative multi-tissue profiling reveals extensive tissue-specificity in transcriptome reprogramming during thermal adaptation, ELife 17 11 (2022) e78556, https://doi.org/10.7554/eLife.78556.
[19] Y. Hayashi, I. Shimizu, Y. Yoshida, R. Ikegami, M. Suda, G. Katsuumi, et al., Coagulation factors promote brown adipose tissue dysfunction and abnormal systemic metabolism in obesity, IScience 25 (7) (2022) 104547, https://doi.org/10.1016/j.isci.2022.104547.
[20] F. Villarroya, R. Cereijo, J. Villarroya, M. Giralt, Brown adipose tissue as a secretory organ, Nat. Rev. Endocrinol. 13 (1) (2017) 26–35, https://doi.org/10.1038/nrendo.2016.136.
[21] R.J. Samms, G.F. Zhang, W. He, O. Ilkayeva, B.A. Droz, S.M. Bauer, et al., Tirzepatide induces a thermogenic-like amino acid signature in brown adipose tissue, Mol. Metab. 64 (2022) 101550, https://doi.org/10.1016/j.molmet.2022.101550.
[22] T. Coskun, K.W. Sloop, C. Loghin, J. Alsina-Fernandez, S. Urva, K.B. Bokvist, et al., LY3298176, a novel dual GIP and GLP-1 receptor agonist for the treatment of type 2 diabetes mellitus: From discovery to clinical proof of concept, Mol. Metab. 18 (2018) 3–14, https://doi.org/10.1016/j.molmet.2018.09.009.
[23] E. Ravussin, G. Sanchez-Delgado, C.K. Martin, R.A. Beyl, F.L. Greenway, L. S. O'Farrell, et al., Tirzepatide did not impact metabolic adaptation in people with obesity, but increased fat oxidation, Cell Metab. 37 (5) (2025) 1060–1074.e4, https://doi.org/10.1016/j.cmet.2025.03.011.
[24] D. Beiroa, M. Imbernon, R. Gallego, A. Senra, D. Herranz, F. Villarroya, et al., GLP-1 agonism stimulates brown adipose tissue thermogenesis and browning through hypothalamic AMPK, Diabetes 63 (10) (2014) 3346–3358, https://doi.org/10.2337/db14-0302.
[25] J.L. Beaudry, K.D. Kaur, E.M. Varin, L.L. Baggio, X. Cao, E.E. Mulvihill, et al., Physiological roles of the GIP receptor in murine brown adipose tissue, Mol. Metab. 28 (2019) 14–25, https://doi.org/10.1016/j.molmet.2019.08.006.
[26] S.A. Lyons, M.B.S. Lea, M. Parikh, Z. Guo, S. Kagdi, A.R. Bisnauth, et al., Acute exogenous acyl-GIP treatment enhances lipid handling and fatty acid oxidation by involving brown fat, EMBO Rep. 26 (21) (2025) 5154–5171, https://doi.org/10.1038/s44319-025-00582-7.
[27] S. Wueest, E.J. Schoenle, D. Konrad, Depot-specific differences in adipocyte insulin sensitivity in mice are diet- and function-dependent, Adipocyte 1 (3) (2012) 153–156, https://doi.org/10.4161/adip.19910.
[28] J.C. Chang, S. Durinck, M.Z. Chen, N. Martinez-Martin, J.A. Zhang, I. Lehoux, et al., Adaptive adipose tissue stromal plasticity in response to cold stress and antibody-based metabolic therapy, Sci. Rep. 9 (1) (2019) 8833, https://doi.org/10.1038/s41598-019-45354-1.
[29] W. Shin, Y. Okamatsu-Ogura, S. Matsuoka, A. Tsubota, K. Kimura, Impaired adrenergic agonist-dependent beige adipocyte induction in obese mice, J. Vet. Med. Sci. 81 (6) (2019) 799–807, https://doi.org/10.1292/jvms.19-0070.
[30] K. El, J.D. Douros, F.S. Willard, A. Novikoff, A. Sargsyan, D. Perez-Tilve, et al., The incretin co-agonist tirzepatide requires GIPR for hormone secretion from human islets, Nat. Metab. 5 (6) (2023) 945–954, https://doi.org/10.1038/s42255-023-00811-0.
[31] H.J. van Eyk, E.H.M. Paiman, M.B. Bizino, S.L. IJzermans, F. Kleiburg, T.G. W. Boers, et al., Liraglutide decreases energy expenditure and does not affect the fat fraction of supraclavicular brown adipose tissue in patients with type 2 diabetes, Nutr. Metab. Cardiovasc. Dis. NMCD 30 (4) (2020) 616–624, https://doi.org/10.1016/j.numecd.2019.12.005.
[32] L.G.M. Janssen, K.J. Nahon, K.F.M. Bracké, D. van den Broek, R. Smit, A.S. D. Sardjoe Mishre, et al., Twelve weeks of exenatide treatment increases [18F] fluorodeoxyglucose uptake by brown adipose tissue without affecting oxidative resting energy expenditure in nondiabetic males, Metab. Clin. Exp. 106 (2020) 154167, https://doi.org/10.1016/j.metabol.2020.154167.
[33] D.B. Harrison, A.L. Phillips, J.B. Tansey, T.J. Clarke, C.B. Wood, L. Nedzi, et al., Brown adipose tissue mimicking head and neck cancer on PET scan in a patient on GLP-1 drug, Laryngoscope 135 (2) (2025) 741–743, https://doi.org/10.1002/lary.31815.
[34] S.M.N. Heimbürger, B. Hoe, C.N. Nielsen, N.C. Bergman, K. Skov-Jeppesen, B. Hartmann, et al., GIP affects hepatic fat and brown adipose tissue thermogenesis but not white adipose tissue transcriptome in type 1 diabetes, J. Clin. Endocrinol. Metab. 107 (12) (2022) 3261–3274, https://doi.org/10.1210/clinem/dgac542.
[35] R. Herman, M. Jensterle, S. Horvat, L. Lezaic, Z. Snoj, I. Pusnik, et al., Effect of tirzepatide-induced weight loss on adipose tissue in obesity: rationale and design of the randomized placebo-controlled Tirzepatide Brown and Beige Adipose Tissue Activation (TABFAT) trial, Trials 26 (1) (2025) 300, https://doi.org/10.1186/s13063-025-09045-9.
[36] K.Y. Chen, A.M. Cypess, M.R. Laughlin, C.R. Haft, H.H. Hu, M.A. Bredella, et al., Brown adipose reporting criteria in imaging studies (BARCIST 1.0): recommendations for standardized FDG-PET/CT experiments in humans, Cell Metab. 24 (2) (2016) 210–222, https://doi.org/10.1016/j.cmet.2016.07.014.
[37] M. Chondronikola, P. Annamalai, T. Chao, C. Porter, M.K. Saraf, F. Cesani, et al., A percutaneous needle biopsy technique for sampling the supraclavicular brown adipose tissue depot of humans, Int. J. Obes. (2005) 39 (10) (2015) 1561–1564, https://doi.org/10.1038/ijo.2015.76.
[38] J. Law, D.E. Morris, C. Izzi-Engbeaya, V. Salem, C. Coello, L. Robinson, et al., Thermal imaging is a noninvasive alternative to PET/CT for measurement of brown adipose tissue activity in humans, J. Nucl. Med. Off. Publ. Soc. Nucl. Med. 59 (3) (2018) 516–522, https://doi.org/10.2967/jnumed.117.190546.
[39] I. Gómez-García, J. Trepiana, A. Fernández-Quintela, M. Giralt, M.P. Portillo, Sexual dimorphism in brown adipose tissue activation and white adipose tissue browning, Int. J. Mol. Sci. 26 23 (15) (2022) 8250, https://doi.org/10.3390/ijms23158250.